Pure Appl. Chem., Vol. 85, No. 7, pp. 1427–1435, 2013.
http://dx.doi.org/10.1351/PAC-CON-12-12-07

Electric-field effects on photoinduced dynamics and function*

Nobuhiro Ohta

Research Institute for Electronic Science, Hokkaido University, Sapporo 001-0020, Japan

Abstract: Photoinduced electron-transfer processes are enhanced or quenched by application of electric fields, depending on the donor–acceptor pairs. Electric-field-induced quenching of photoluminescence, which results from the field-induced dissociation of the exciton state that depends on the photoexcitation wavelength, is observed in π-conjugated polymers. These electric-field effects on photoinduced dynamics have been confirmed by the measurements both of electroabsorption and electrophotoluminescence spectra and of time-resolved electrophotoluminescence decays. Time-resolved measurements of photocurrent, with which novel material function in electrical conductivity of organic materials induced by photoirradiation and application of electric fields is confirmed, are also reviewed.

Keywords: electric-field effects; electrophotoluminescence spectrum; photoinduced electron transfer; photoinduced phase transition.

INTRODUCTION

Electroabsorption (E-A) and electrophotoluminescence spectroscopy, where electric-field-induced change in absorption and photoluminescence spectra is measured, is a powerful method to examine the electric-field effect on photoinduced dynamics as well as the change in electronic structure following optical transition [1–4]. By combining this method with the time-resolved measurements both of the photoluminescence decay profile and of its field-induced change, we can examine how photoinduced dynamics is influenced by application of electric fields [5]. Here, some results of the electric-field effects on photoinduced dynamics will be introduced.

As a result of the field-induced change in molecular motion and photoinduced dynamics, novel property and function of materials in electrical property can be generated by photoirradiation and application of electric fields. Time-resolved photoresponses of electrical conductivity measured by synchronizing the excitation laser pulse with the pulsed voltage show that insulator-to-metal transition (ITMT) is induced by a combination of photoirradiation and application of electric fields in some organic crystals [6].

ELECTROPHOTOLUMINESCENCE SPECTRA

The state energy of molecules is influenced by an electric field ($\boldsymbol{F}$), depending on the magnitude of the electric dipole moment $\boldsymbol{\mu}$ and the molecular polarizability $\boldsymbol{\alpha}$ in the states under consideration, that is, the state is shifted by E (= $-\boldsymbol{\mu}\cdot\boldsymbol{F} - \boldsymbol{F}\cdot\boldsymbol{\alpha}\cdot\boldsymbol{F}/2$) [1–4]. As a result, the field-induced change in transition

Pure Appl. Chem.* **85, 1257–1513 (2013). A collection of invited papers based on presentations at the XXIVth IUPAC Symposium on Photochemistry, Coimbra, Portugal, 15–20 July 2012.

energy between the ground and excited states (ΔE) is given by $-\boldsymbol{\Delta\mu}\cdot\boldsymbol{F} - \boldsymbol{F}\cdot\boldsymbol{\Delta\alpha}\cdot\boldsymbol{F}/2$, where $\boldsymbol{\Delta\mu}$ and $\boldsymbol{\Delta\alpha}$ are the differences in dipole moment and molecular polarizability, respectively, between two states where optical transition occurs. In randomly distributed systems (i.e., by assuming an isotropic angular distribution of molecules without external electric field), electrophotoluminescence spectra (i.e., plots of the field-induced change in photoluminescence intensity (ΔI_{PL}) as a function of wavenumber ν), are given by the following equation [4]:

$$\Delta I_{PL}(\nu) = (f\boldsymbol{F})^2\left[AI_{PL}(\nu) + B\nu^3\frac{d}{d\nu}\left\{\frac{I_{PL}(\nu)}{\nu^3}\right\} + C\nu^3\frac{d^2}{d\nu^2}\left\{\frac{I_{PL}(\nu)}{\nu^3}\right\}\right] \quad (1)$$

Here, I_{PL} is photoluminescence intensity, A, B and C are coefficients, and f is internal field factor. Hereafter, photoluminescence and electrophotoluminescence are abbreviated by PL and E-PL, respectively. The first and second derivative components in eq. 1 mainly arise from $\boldsymbol{\Delta\alpha}$ and $\boldsymbol{\Delta\mu}$, respectively, between the emitting state and the ground state. If the polarizability change $\boldsymbol{\Delta\alpha}$ is significant, the Stark shift of the transition energy results in the red- or blue-shift of the PL spectra, giving the E-PL spectra having the same shape as that of the first derivative of the PL spectra. If the dipole moment change $\boldsymbol{\Delta\mu}$ is significant, the Stark shift of the transition energy results in the broadening of the PL spectra, giving the E-PL spectra having the same shape as that of the second derivative of the PL spectra. E-A spectrum (i.e., plots of the field-induced change in absorption spectrum) is also given by a linear combination of the zeroth, first, and second derivatives of absorption spectrum [1–3,7], and the first and second derivative components mainly arise from $\boldsymbol{\Delta\alpha}$ and $\boldsymbol{\Delta\mu}$, respectively, as in the case of E-PL spectrum. The zeroth derivative component of the E-A spectra results from the field-induced change in transition moment and field-induced molecular reorientation [1–3,7,8]. On the other hand, the zeroth derivative component of the E-PL spectra in eq. 1 corresponds to the field-induced change in emission quantum yield. Then, electric-field effects on photoinduced dynamics can be evaluated from the zeroth derivative component of the E-PL spectra.

The change in emission quantum yield may arise from the field-induced change in radiative decay rate and/or nonradiative decay rate of the emitting state. The field-induced change in emission intensity also occurs when the population of the emitting state following optical excitation is affected by application of electric field. In order to understand which mechanism plays an important role, direct measurements of the field-induced change in time-resolved emission decay profile are necessary. Another caution must be paid that the field-induced change in emission intensity also comes from the change in absorption intensity. In our experiments, excitation was done at wavelengths where the change in absorption intensity was negligible, unless otherwise noted, since the change in PL which comes from the change in absorption intensity is not essential to discuss the field effect on dynamics.

ELECTRIC-FIELD EFFECTS ON PHOTOINDUCED DYNAMICS

Field-induced change in photoinduced electron transfer (PIET)

It has been confirmed that PIET is significantly influenced by application of electric fields. Electron-transfer rate usually depends on the free energy gap between reactant and product and on the electronic coupling between donor and acceptor, as shown by the Marcus theory [9,10]. Because of the large electric dipole moment of the radical ion pair (RIP) produced by electron transfer, the energy level of the product (i.e., RIP) is expected to be significantly shifted by application of electric field. Then it is expected that the initial step of the electron-transfer process is influenced by electric fields. Since the emission process competes with nonradiative processes including electron transfer, electric-field effect on the initial step of electron transfer can be detected as a field-induced change of the PL intensity. If PIET is accelerated (decelerated) by application of electric fields, emission from the state where electron transfer occurs will be quenched (enhanced). In fact, the electric-field effect on PIET could be con-

firmed in a variety of linked or unlinked pairs of electron donor and acceptor, which are arranged with a well-defined molecular order, where PIET occurs with a definite direction, and which are randomly distributed, based on the E-A and E-PL measurements. As the well-ordered samples, Langmuir–Blodgett (LB) films were used to prepare such a molecular system [11,12]. As the randomly distributed samples, pairs of pyrene and dimethylaniline, carbazole and dimethyl-terephthalate, phenanthrene and phthalimide, pyrene and *N*-methylphthalimide, phenanthrene and *N*,*N*-dimethylaniline, porphyrin and C_{60} were taken, and electric-field effects on PIET have been examined in poly(methyl methacrylate) (PMMA) [13–21].

Here, the results of the pair of porphyrin and C_{60} are introduced. Figure 1 shows the E-PL spectra both of the linked compound of zinc porphyrin and C_{60} (ZnP-C_{60}) and of the linked compound of free-base porphyrin and C_{60} (H_2P-C_{60}), whose molecular structure is shown in the figure [22], together with the PL spectrum. In the presence of $\boldsymbol{F}$, PL emitted from the locally excited state of porphyrin is quenched in H_2P-C_{60}, whereas PL is enhanced in ZnP-C_{60}, as shown in Fig. 1. At the emitting state of porphyrin, the emission process is considered to compete with the electron transfer to C_{60}. Then, the field-induced quenching or the field-induced enhancement of PL suggests that the electron transfer from the excited state of porphyrin is accelerated or decelerated by application of $\boldsymbol{F}$, respectively. In fact, the electric-field effects on PL decay profile support the conclusion, as shown in Fig. 2, where PL decay profiles observed both in the absence and in the presence of $\boldsymbol{F}$ are shown, together with the ratio between two decay profiles. At the initial stage of time, the ratio is unity, indicating that the PL intensity as well as population of the emitting state is not affected by application of $\boldsymbol{F}$. As a passage of time, the ratio becomes larger in ZnP-C_{60} (i.e., the lifetime becomes longer), whereas the ratio becomes smaller in H_2P-C_{60} (i.e., the lifetime becomes shorter). These results clearly show that electron transfer from the excited state of porphyrin chromophore to C_{60} is accelerated in H_2P-C_{60} and decelerated in ZnP-C_{60} in the presence of $\boldsymbol{F}$, indicating that the electric-field effect on PIET depends on the donor–acceptor pair.

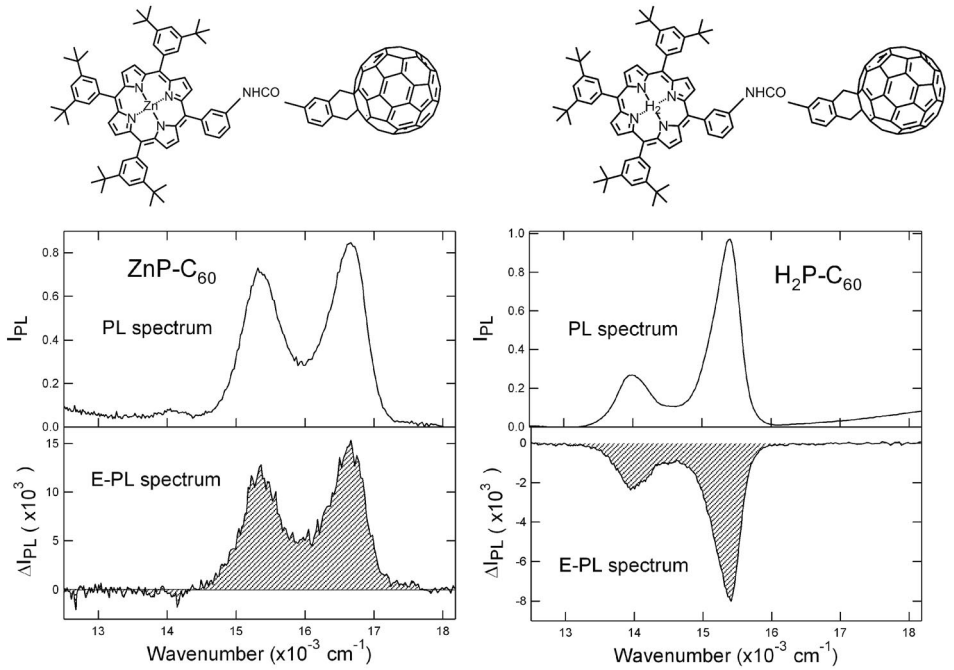

Fig. 1 PL spectra (upper) and E-PL spectra (lower) of ZnP-C_{60} (left) and H_2P-C_{60} (right) in a PMMA film. Molecular structure is also shown. In both cases, the applied field strength was 1.0 MV cm^{-1}.

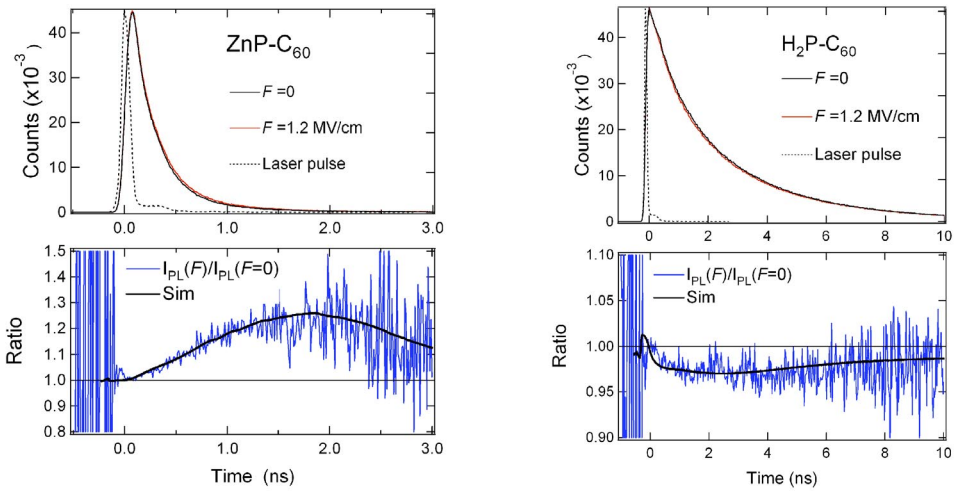

Fig. 2 (Upper) PL decays at zero field and at 1.2 MV cm^{-1}, together with the pulse shape of the scattered laser light, (lower) ratio of the decay in the presence of ***F*** relative to that at zero field for ZnP-C_{60} (left) and H_2P-C_{60} (right) in a PMMA film.

According to the Marcus theory, the rate constant of electron transfer depends on the energy gap (ΔG_0) as well as on the reorganization energy (λ), and the barrier height for the electron transfer (ΔG^*) is given by $(\lambda + \Delta G_0)^2/4\lambda$ [23]. Note that ΔG_0 is given by $\Delta G - e^2/(\varepsilon_s r)$, where ΔG, r, e, and ε_s are the standard Gibbs free energy gap of the reaction, donor–acceptor distance, the charge of electron, and dielectric constant of the matrix, respectively. Note that ΔG is estimated to be –0.45 eV for ZnP-C_{60} and –0.05 eV for H_2P-C_{60}, respectively, with reference to the equation of Weller [19,24]. If the value of λ is assumed to be 0.6 eV [22], the barrier height is estimated to be ~1×10^{-2} eV in ZnP-C_{60} and ~1×10^{-1} eV in H_2P-C_{60}, suggesting that the electron transfer in ZnP-C_{60} is much faster than the other because of the small barrier height. In fact, the fluorescence lifetime observed in PMMA is much shorter in ZnP-C_{60} than the other, that is, ~ 200 ps in ZnP-C_{60} and ~2.0 ns in H_2P-C_{60} (cf. the decay profiles shown in Fig. 2). Then, the opposite behavior of the electric-field effect on fluorescence between ZnP-C_{60} and H_2P-C_{60} can be interpreted as follows (see Fig. 3): The barrier height for PIET (i.e., ΔG^*) is much smaller in ZnP-C_{60} than that in H_2P-C_{60}, as known from the fluorescence lifetime, and the field-induced decrease of the rate of PIET occurs in the "barrier-free regime" where the barrier

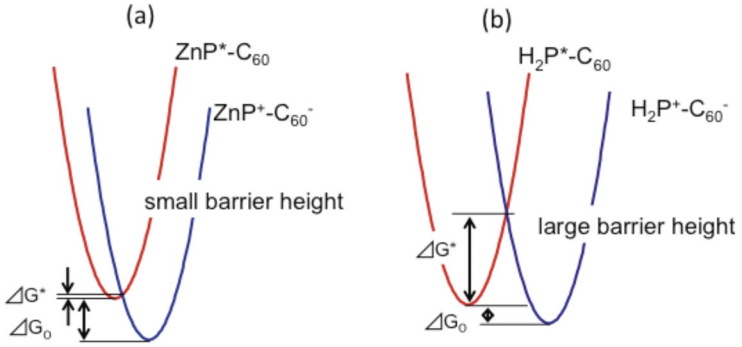

Fig. 3 Possible relation of the original potential energy surface between reactant and product of electron donor and acceptor pairs of ZnP-C_{60} (left) and H_2P-C_{60} (right). ZnP* (H_2P*) shows the electronically excited state.

height is very small. In the case where the barrier-height for PIET is large (i.e., in H_2P-C_{60}), on the other hand, field-induced increase of the electron-transfer occurs, which leads to the field-induced quenching of PL.

Electric-field effect on the rate of PIET also depends on the donor–acceptor distance, as shown in methylene-linked compound of carbazole and terephthalic acid methyl ester [25]. The mechanism of the distance dependence of the electric-field effect on the electron-transfer rate has been shown theoretically [26].

Field-induced change in photoinduced dynamics of π-conjugated polymers

Photoinduced dynamics of π-conjugated polymers such as poly(9,9-dioctylfluorene) (PFO) and poly(*p*-phenylene vinylene) (PPV) derivatives is also affected by application of electric field, depending on the excitation wavelength and the applied field strength. Here, the results of PFO are introduced [27]. PL spectra as well as E-PL spectra of PFO with excitation at 344 and 298 nm are shown in Fig. 4. The PL spectra, which were independent of the excitation wavelength, are assigned to the fluorescence emitted from β-phase of PFO [28]. With excitation at a longer wavelength of 344 nm, the E-PL spectra observed with a field strength of 0.4 MV cm^{-1} shows the same shape as the one of the first derivative of the PL spectrum, indicating the Stark shift resulting from the difference in molecular polarizability between the emitting state and the ground state. When the field strength was rather weak, the field-induced change in intensity was not observed at the longer wavelength excitation, indicating that the dynamics of PFO following photoexcitation is not affected by application of $\boldsymbol{F}$. As the applied field becomes stronger, however, the shape of the E-PL spectrum becomes similar to the one of the PL spectrum, and the integrated intensity of the E-PL spectrum becomes negative, indicating that the emission quantum yield becomes smaller by application of strong electric fields even with excitation at a longer wavelength of 344 nm. With excitation into higher excited states, PL of PFO is quenched by $\boldsymbol{F}$ even with a low field of 0.4 MV cm^{-1}, and the magnitude of the quenching increases with increasing the applied field strength, as shown in Fig. 4.

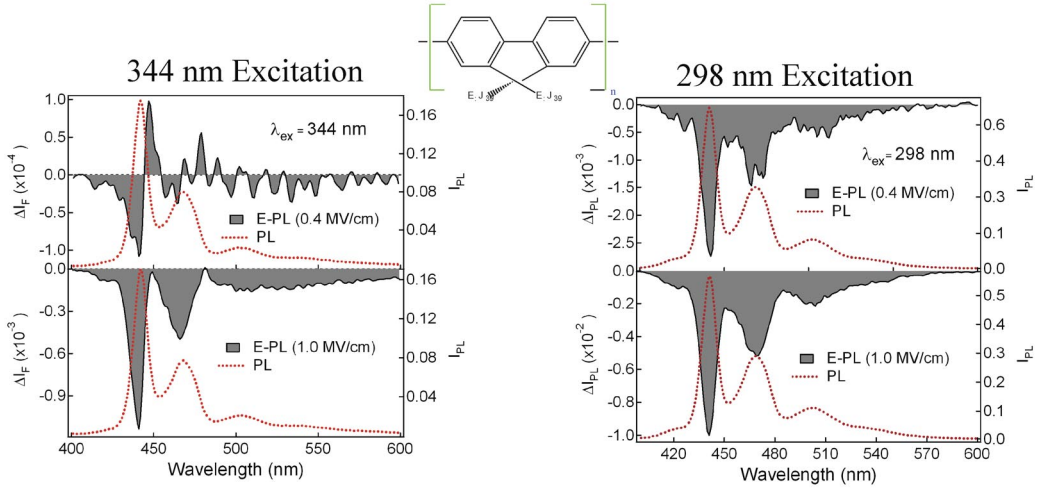

Fig. 4 PL spectra (dotted line) and E-PL spectra (shaded line) of PFO film with 344 nm excitation (left) and 298 nm excitation (right). Applied field strength was 0.4 MV cm^{-1} (upper) and 1.0 MV cm^{-1} (below).

In order to confirm whether the field-induced quenching of PL results from an increased nonradiative decay rate of the emitting state, which leads to a decrease of the emission lifetime, or from

a decreased initial population of the excited species at the emitting state following optical excitation, the field-induced change in emission decay profiles of PFO was measured. The decay profiles at zero field [$I_{PL}(\boldsymbol{F} = 0)$] and in the presence of $\boldsymbol{F}$ at 0.6 or 1.0 MV cm^{-1} [$I_{PL}(\boldsymbol{F})$] and the ratio between those decay profiles, i.e., $I_{PL}(\boldsymbol{F})/I_{PL}(\boldsymbol{F} = 0)$, were measured with excitation at 298 nm. The results are shown in Fig. 5. If the initial population of the emitting state is not affected by $\boldsymbol{F}$, the ratio of $I_{PL}(\boldsymbol{F})/I_{PL}(\boldsymbol{F} = 0)$ must be unity just after photoexcitation. If the emission lifetime is independent of $\boldsymbol{F}$, $I_{PL}(\boldsymbol{F})/I_{PL}(\boldsymbol{F} = 0)$ must be constant over the entire time domain. As shown in Fig. 5, the ratio is less than unity just after photoexcitation and roughly constant in the whole time region, indicating that the emission lifetime is not affected by $\boldsymbol{F}$ significantly. Emission shows a nearly single exponential decay given by $a \exp(-t/\tau)$, and the lifetime, i.e., τ, was 311 ps at zero field. Actually, the ratio of the decay in the presence of $\boldsymbol{F}$ relative to the decay at zero field slightly increases as a passage of time, as shown in Fig. 5, indicating that the average lifetime slightly increases in the presence of $\boldsymbol{F}$. When the pre-exponential factor, a, at zero field is normalized to unity, it was determined from the simulation that the pre-exponential factors at 0.6 and 1.0 MV cm^{-1} were 0.980 and 0.949, respectively, and the lifetime was 312 ps in both cases. Note that the decay profile and the ratio between two decays at zero field and in the presence of $\boldsymbol{F}$ simulated by assuming a single exponential function are shown in Fig. 5. Then, the field-induced quenching of PL is attributed to the field-induced decrease in the population of the fluorescent PFO just after photoexcitation. The quenching observed at high fields irrespective of excitation wavelength is ascribed to the field-assisted generation of hole-electron pairs followed by efficient charge transport. The field-induced quenching observed at rather weak fields, which is more efficient at shorter wavelength excitation, may be ascribed to the field-induced enhancement of the electron transfer, which occurs from highly excited state through the π-conjugated polymer chain [27]. Similar electric-field effects on PL intensity and decay were observed in other π-conjugated polymers such as PPV derivatives [29,30].

It is noted that the field-assisted dissociation of the photoexcited state, which leads to the field-induced quenching of PL, also occurs in semiconductor quantum dots such as CdS or CdTe nanoparticles [31,32].

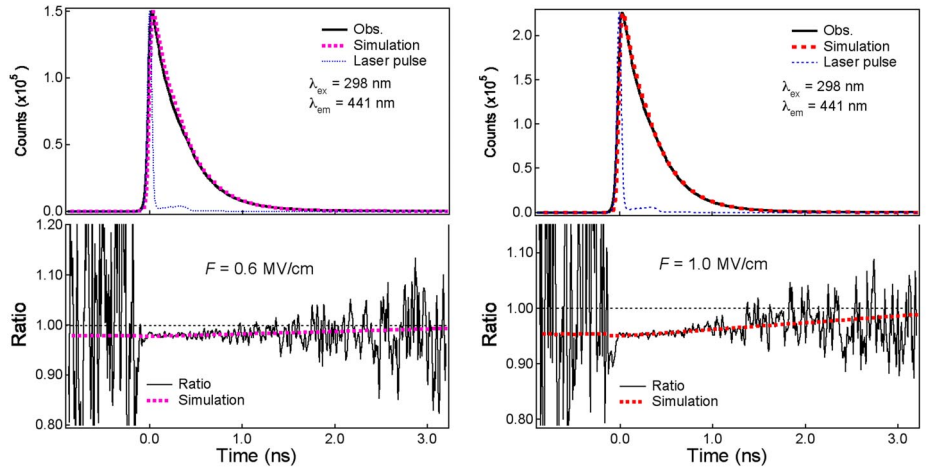

Fig. 5 (Upper) Observed and simulated PL decay profiles of PFO film, and the pulse shape of the scattered laser light, (lower) ratio of the decay profile in the presence of $\boldsymbol{F}$ relative to that at zero field (solid line), together with the simulated one (dotted line). The applied field strength was 0.6 MV cm^{-1} in the left and 1.0 MV cm^{-1} in the right. Excitation and observation wavelengths were 298 and 441 nm, respectively.

EFFECTS OF PHOTOIRRADIATION AND APPLICATION OF ELECTRIC FIELD ON ELECTRICAL CONDUCTIVITY

Novel property and function of materials may be induced by photoirradiation and application of electric fields, as a result of the field-induced change both in photoinduced dynamics of molecules and in molecular motion. In order to examine the effects of photoirradiation and application of electric fields on electrical conductivity, time-resolved photoresponse has been measured by synchronizing the excitation laser pulse with a pulsed voltage. We have focused on the organic charge-transfer compounds consisting of the planar donor molecule BEDT-TTF, which is bis(ethylenedithio)tetrathiafulvalene, and counter anion, in the hope that simultaneous application of photoirradiation and electric field induces novel function in electrical conductivity. As a light source, a Nd:YAG laser or an optical parametric oscillator unit mounting a β-barium borate (BBO) crystal pumped by a third harmonic of the output of a pulsed Nd:YAG laser was used. The pulse width of the output was ~10 ns. Then, the synergy effect of photoirradiation and applied electric field on electric conductivity was found with the irradiation light of 532 nm in single crystals of α-$(BEDT\text{-}TTF)_2I_3$, which is hereafter denoted by α-I_3 [33].

The photocurrent time profiles of α-I_3 observed with a pulsed voltage having height of 3.0 or 8.0 V and width of 4 ms at 115 K, where the sample was in the insulating charge-ordered state, are shown in Figs. 6a and 6b, respectively. Without photoirradiation, a flat current profile coming from the dark resistance of ~1×10^5 Ω was observed. With photoirradiation at the light intensity of 3.4×10^{-5} J/pulse, a high current was observed during the application of the pulsed voltage (see Fig. 6b), indicating the conductivity switching from the low-conductivity (LC) state to the high-conductivity (HC) state, i.e., ITMT, is induced by photoirradiation. It is noted that ITMT occurs with photoirradiation with applied voltages larger than the threshold value [33]. Photoirradiated crystals show differential negative resistance [30], and bistability (i.e., hysteresis loop) was observed in the *I–V* characteristic curve, as shown in Fig. 6c, which shows the plots obtained by scanning the pulsed voltage height in the positive and negative directions with photoirradiation at the same intensity. The current observed at the end of the duration of applied pulsed voltage was used as the current in Fig. 6c. ITMT occurs with photoirradiation where light intensity is larger than the threshold value, and bistability was also observed in the plots of current vs. irradiation light intensity; the light intensity required for the LC-to-HC switching (i.e., ITMT) is larger than that for the switching from HC state to LC state in the scanning of the light intensity from the high intensity to the low intensity. The photoinduced HC state could be repeatedly recovered by applying the pulsed voltages without further photoirradiation, depending on the pulse width of the applied voltage, even after the current was reduced to zero, indicating a memory effect in the photoinduced conductivity switching [33]. The threshold in width and height of the pulsed voltage for the memory effect can be controlled by irradiation light intensity. These results clearly show that the

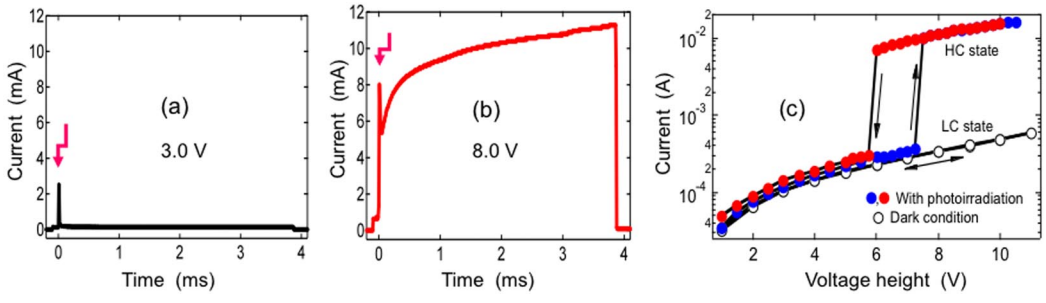

Fig. 6 A current profile measured at 115 K induced by photoirradiation with a pulsed voltage height of 3.0 V (a) and 8.0 V (b), and the *I–V* characteristic curves obtained by scanning the height of the pulsed voltage in the positive and negative directions at 115 K with and without photoirradiation (c). The arrow in (a) and (b) corresponds to the laser pulse.

electrical conductivity of organic materials can be controlled by photoirradiation and application of the pulsed voltage (pulsed electric field).

Similar photoinduced ITMT, which shows the synergy effect of photoirraditiaon and application of electric field on electrical conductivity, was also observed in single crystals of deuterated κ-(BEDT-TTF)$_2$Cu[N(CN)$_2$]Br [34].

CONCLUSION AND OUTLOOK

E-PL spectra, time-resolved E-PL decay, and E-A spectra were measured for various types of molecules and molecular systems such as electron donor–acceptor pairs, which show PIET, and π-conjugated polymers. Based on the results, electric-field effects on excitation dynamics following optical transitions have been examined. In the result, PIET was confirmed to be significantly influenced by application of electric fields. Photoinduced dynamics of π-conjugated polymers was also confirmed to be significantly influenced by application of the electric field, depending on the excitation energy.

By combining the nanosecond laser pulse with pulsed voltage, time-resolved photocurrents have been measured in organic donor–acceptor complexes, and the photoirradiation effect and electric-field effect effect on electrical conductivity have been examined. Then, photoinduced ITMT, which depends on irradiation light intensity and on the height and width of the applied pulsed voltage, has been observed in single crystals of α-(BEDT-TTF)$_2$I$_3$ and deuterated κ-(BEDT-TTF)$_2$Cu[N(CN)$_2$]Br. Thus, it is expected that the novel functionality of materials can be generated by a combination of photoirradiation and application of electric field. In analogy with the so-called internal photoelectric effect, where material conductivity is changed by photoirradiation, the search and quests for novel functional materials using photoirradiation and application of the external electric field may lead to a new research field, called *photoelectrics*.

ACKNOWLEDGMENTS

I would like to thank all the co-workers, who are listed in the references as the co-authors, for their invaluable contribution, support, and discussion.

REFERENCES

1. W. Liptay. In *Excited State*, Vol. 1, E. C. Lim (Ed.), p. 129, Academic Press (1974).
2. G. U. Bublitz, S. G. Boxer. *Ann. Rev. Phys. Chem.* **48**, 213 (1997).
3. F. W. Vance, R. D. Williams, J. T. Hupp. *Int. Rev. Phys. Chem.* **17**, 307 (1998).
4. N. Ohta. *Bull. Chem. Soc. Jpn*. **75**, 1637 (2002).
5. M. Tsushima, T. Ushizaka, N. Ohta. *Rev. Sci. Instrum*. **75**, 479 (2004).
6. T. Iimori, T. Naito, N. Ohta. In *Molecular Electronic and Related Materials – Control and Probe with Light*, Chap. 8, p. 167, Transworld Research Network (2010).
7. E. Jalviste, N. Ohta. *J. Photochem. Photobiol. C: Photochem. Rev.* **8**, 30 (2007).
8. S. L. Locknar, A. Chowdhury, L. A. Peteanu. *J. Phys. Chem. B* **104**, 5816 (2000).
9. (a) R. A. Marcus. *J. Chem. Phys*. **24**, 966 (1956); (b) R. A. Marcus. *Ann. Rev. Phys. Chem*. **15**, 155 (1964).
10. R. A. Marcus, N. Sutin. *Biochem. Biophys. Acta* **811**, 265 (1985).
11. T. Ito, I. Yamazaki, N. Ohta. *Chem. Phys. Lett.* **277**, 125 (1997).
12. N. Ohta, T. Ito, I. Yamazaki. *Z. Phys. Chem.* **213**, Part II, 191 (1999).
13. M. Tsushima, N. Ohta. *J. Chem. Phys.* **120**, 6238 (2004).
14. N. Ohta, M. Koizumi, S. Umeuchi, Y. Nishimura, I. Yamazaki. *J. Phys. Chem.* **100**, 16466 (1996).
15. T. Iimori, T. Yoshizawa, T. Nakabayashi, N. Ohta. *Chem. Phys.* **319**, 101 (2005).
16. H. Kawabata, N. Ohta. *J. Chem. Phys*. **114**, 7723 (2001).

17. H. Kawabata, Y. Nishimura, I. Yamazaki, K. Iwai, N. Ohta. *J. Phys. Chem. A* **105**, 10261 (2001).
18. T. Yoshizawa, M. Mizoguchi, T. Iimori, T. Nakabayashi, N. Ohta. *Chem. Phys.* **324**, 26 (2006).
19. N. Ohta, S. Mikami, Y. Iwaki, M. Tsushima, H. Imahori, K. Tamaki, Y. Sakata, S. Fukuzumi. *Chem. Phys. Lett.* **368**, 230 (2003).
20. Md. Wahadoszamen, T. Nakabayashi, S. Kang, H. Imahori, N. Ohta. *J. Phys. Chem. B* **110**, 20354 (2006).
21. N. Ohta. *ECS Trans.* **6**, 3 (2007).
22. H. Imahori, K. Hagiwara, M. Aoki, T. Akiyama, S. Taniguchi, T. Okada, M. Shirakawa, Y. Sakata. *J. Am. Chem. Soc.* **118**, 11771 (1996).
23. G. J. Kavaros. *Fundamentals of Photoinduced Electron Transfer*, Wiley-VCH, New York (1993).
24. A. Weller. *Z. Phys. Chem. NF* **133**, 93 (1982).
25. T. Kanada, Y. Nishimura, I. Yamazaki, N. Ohta. *Chem. Phys. Lett.* **332**, 442 (2000).
26. M. Hilczer, M. Tachiya. *J. Chem. Phys.* **117**, 1759 (2002).
27. M. S. Mehata, C.-S. Hsu, Y.-P. Lee, N. Ohta. *J. Phys. Chem. C* **113**, 11907 (2009).
28. T. Tunno, A. P. Caricato, M. E. Caruso, A. Luches, M. Martino, F. Romano, D. Valerini, M. Anni. *Appl. Surf. Sci.* **253**, 6461 (2007).
29. (a) M. S. Mehata, C.-S. Hsu, Y.-P. Lee, N. Ohta. *J. Phys. Chem. B* **114**, 6258 (2010); (b) M. S. Mehata, C.-S. Hsu, Y.-P. Lee, N. Ohta. *J. Phys. Chem. C* **116**, 14789 (2012).
30. M. Esteghamatian, Z. D. Popovic, G. Xu. *J. Phys. Chem.* **100**, 13716 (1996).
31. Y. Ohara, T. Nakabayashi, K. Iwasaki, T. Torimoto, B. Ohtani, T. Hiratani, K. Konishi, N. Ohta. *J. Phys. Chem. B* **110**, 20927 (2006).
32. R. Ohshima, T. Nakabayashi, Y. Kobayashi, N. Tamai, N. Ohta. *J. Phys. Chem. C* **115**, 15274 (2011).
33. (a) T. Iimori, T. Naito, N. Ohta. *J. Am. Chem. Soc.* **129**, 3486 (2007); (b) T. Iimori, T. Naito, N. Ohta. *Appl. Phys. Lett.* **90**, 262103 (2007); (c) T. Iimori, T. Naito, N. Ohta. *J. Phys. Chem. C* **113**, 4654 (2009).
34. F. Sabeth, T. Iimori, N. Ohta. *J. Am. Chem. Soc.* **134**, 6984 (2012).

